Bioenerg. Res. (2014) 7:1253–1269
DOI 10.1007/s12155-014-9462-4

Simulation of Biomass and Nitrogen Dynamics in Perennial Organs and Shoots of *Miscanthus*×*Giganteus* Using the STICS Model

L. Strullu · N. Beaudoin · I. G. de Cortàzar Atauri · B. Mary

Published online: 3 May 2014

Abstract Biomass production by perennial plants promises to increase land use efficiency and reduce greenhouse gas emissions from cropping systems dedicated to bioenergy production. The modelling of both biomass production and the environmental impacts of these systems over the long term is needed in order to evaluate their sustainability. New equations have been added to the STICS soil-crop-atmosphere model to provide a better description of perennial organs and their relationship with non-perennial ones, corresponding to the rhizomes and shoots, respectively in the *Miscanthus*× *giganteus* case study. Their description is intended to be generic for perennial plants, supported by the functional approach of STICS. The new version of STICS 8 was calibrated using published data and then validated against independent data. It was able to simulate the biomass and nitrogen content of the shoots (with a model efficiency of 0.95 and 0.70, respectively) and reproduce the dynamic of biomass and nitrogen in perennial organs (with a model efficiency of 0.41 and 0.63, respectively). Some of the model's improvements are discussed. Modifications to the model allowed simulations of the effect of cultural practices, such as nitrogen fertilisation or harvest date, on the biomass and nitrogen content of rhizomes and shoots.

Keywords *Miscanthus* · Model · Remobilisation · Storage · Perennial plant · Bioenergy · STICS

L. Strullu · N. Beaudoin · B. Mary (✉)
INRA, UR1158 AgroImpact, 02000 Barenton-Bugny, France
e-mail: bruno.mary@laon.inra.fr

I. G. de Cortàzar Atauri
INRA, US AgroCilm, Avignon, France

Introduction

In order to reduce anthropogenic greenhouse gas emissions and replace fossil fuels, policies support the use of plant biomass to produce biofuels. The use of dedicated crops for energy production will be useful and acceptable if it provides a real environmental benefit in comparison with fossil fuels. The European Commission (directive 2009/28/CE) has established durability criteria for biofuel production, notably the objective to reduce greenhouse gas emissions by 60 % compared with fossil fuels from 2018. In this case, an evaluation of plant production and environmental impacts has to be done over the long term, particularly for perennial plants which are established for over 15 years. *Miscanthus*× *giganteus* (hereafter referred to as *M. giganteus*) is a promising perennial plant for biomass production due to its high yield potential and low nitrogen requirements [10, 29]. Moreover, *M. giganteus* cropping leads to high carbon inputs in soil organic matter [18].

Modelling is a powerful tool for predicting plant biomass production and its environmental impacts in different agro-environments. Different models have been developed or parameterised in order to simulate biomass production and/or the environmental impacts of crops dedicated to biomass production [32]. There are already five models specifically simulating the biomass production of *M. giganteus* [14, 22, 25, 30, 36]. One recent model has been developed to simulate *M. giganteus* above-ground biomass production with low input data [36], but this model is unable to simulate the plant's environmental impacts. The other models are mechanistic [14, 22, 25, 30] and require more input data concerning plant physiology and phenology. The first mechanistic model, MISCANMOD [14], has been improved to take into account more the impact of temperature and water stress on the plant's radiation use efficiency [22]. This model allows an accurate simulation of the plant's above-ground biomass production by

simulating its decline during winter and the evolution of its moisture content by using empirical relationships [22]. However, this model cannot simulate the biomass in perennial organs, corresponding to the rhizomes for *M. giganteus*, and the nitrogen dynamics in the plant. Two models take into account the biomass of *M. giganteus* perennial organs and are able to simulate above-ground biomass production accurately [25, 30]. Biomass allocation between above-ground and belowground organs is simulated by the dynamic use of partitioning coefficients as a function of plant phenology [25] or at the end of the growing season [30]. However, those models do not take remobilisation processes into consideration or their role in above-ground biomass production during spring growth. Moreover, no existing model [14, 22, 25, 30, 36] is able to simulate nitrogen dynamics in shoots and perennial organs. It is essential to take those dynamics into account in order to assess nitrogen fertiliser requirements and the environmental impacts (nitrate leaching and N_2O emissions) of perennial plants. Conversely, generic models are geared more towards studying environmental impacts than specific models are, allowing a comparison of plant successions [6, 27, 47]. Since they cannot integrate all the characteristics of each species, they need to be carefully calibrated for each new crop. As far as is known, only SWAT, a hydrology-oriented generic model, has been calibrated, but it does not take perennial reserves into account [33].

It is well known that perennial plants use nitrogen and biomass reserves to sustain spring regrowth [31]. Many authors have shown that nitrogen reserves have a substantial impact on the regrowth velocity of perennial plants [3, 42, 43]. The nitrogen stocks of *M. giganteus* perennial organs have a significant impact on nitrogen accumulation in shoots and on plant nitrogen fertilisation needs [39]. They also play a key role in plant biomass production and leaf area index development [40]. As emphasised by Miguez et al. [30], it is a challenge to model yield losses due to leaf senescence, dead leaf drop and biomass storage from shoots in perennial organs of plants such as *M. giganteus*. Modelling biomass storage during the autumn and early winter will allow better simulations of the biomass of harvestable and perennial organs. Moreover, modelling nitrogen remobilisation and storage is essential for simulating the effect of cultivation practices, such as fertilisation or harvest date, on plant biomass production and the environmental impacts over the long term.

The STICS model, a generic and dynamic model simulating the soil-crop-atmosphere system with a daily time step, already simulates some of the role of perennial reserves [7–9]. Its inputs and outputs allow an analysis of the sustainability of different cropping systems via the simulation of biomass production and associated environmental impacts [8]. This information is essential for developing a technically feasible and environmentally sound supply of bioenergy. Input variables relate to climate, soil and plant system and output variables relate to yield and environment, notably in terms of drainage, nitrate leaching, greenhouse gas emissions and the evolution of the C and N stocks in the soil [9]. However, improvements need to be made to the STICS model to simulate perennial plant behaviour over the long term, notably to take into account the nitrogen and biomass dynamic of perennial organs and the evolution of these reserves over the long term.

The aim of this study was to adapt a generic model to the agronomic and environmental assessment of both perennial bioenergy plants and conventional crops. The strategy consisted in (i) adding equations to the STICS plant model (version 8) to simulate biomass and nitrogen dynamics in the two compartments of perennial plants, perennial organs containing reserves with a lifespan exceeding 1 year and non-perennial organs which are renewed each year and (ii) calibrating and validating the model with data from field experiments.

Materials and Methods

The Current STICS Plant Model (V8)

This model was developed to simulate the effect of the climate, soil and plant management on plant growth, development and production (quantity and quality) and on the environment [7]. Plant development is driven by a thermal index (degree-days) or a photothermal index which may or may not take vernalisation into account. The thermal index is used for simulating *M. giganteus* development. Plant growth is driven by the plant's carbon accumulation [17]. Photosynthetic active radiations (PAR) are intercepted by the leaves and transformed into biomass using daily radiation use efficiency according to Beer's law and Monteith's equation. Calculating the water, carbon and nitrogen balances of the soil-plant system every day allows simulations of the effect of water and N stress and their interaction on plant growth. The model simulates the total biomass of the plant and distinguishes the structural biomass of stems, green leaves, dead leaves and the reserves of the plant which are not localised between organs, as described by Brisson et al. [9]. The model simulates the leaf area index dynamic as an equilibrium between the green leaf formation and leaf senescence which occurs when the leaf's lifespan is exceeded. During leaf senescence, biomass remobilisation occurs between dead leaves and reserves.

The plant's nitrogen content depends on the biomass accumulation in shoots and nitrogen availability in the soil. No distinction is made between structural and metabolic nitrogen pools except for the simulation of nitrogen losses due to leaf drop. The model simulates the effect of temperature, water and nitrogen stresses on leaf growth and biomass accumulation using stress indices.

With regard to perennial plants, the model already simulates biomass and nitrogen remobilisation during regrowth [9]. The remobilisation of biomass is limited and driven by the source/sink ratio. It occurs when the daily biomass production is not sufficient to satisfy the plant's carbon requirements. The remobilisation of nitrogen is a function of plant demand and takes priority over nitrogen absorption. Hence, biomass and nitrogen remobilisation occur independently of one another. The lack of compartments and the absence of parallelism between biomass and nitrogen pools simulated by the model mean that it did not accurately simulate biomass and nitrogen dynamics in perennial and non-perennial organs. The model was also unable to simulate biomass and nitrogen remobilisation from non-perennial to perennial organs at the end of the growing season. In the following section, new compartments are described and equations added to the model in order to more realistically simulate biomass and nitrogen dynamics in perennial and non-perennial organs.

Improvement of Biomass and Nitrogen Partitioning Simulations in Perennial Plants

New pools and fluxes were added to the model in order to simulate biomass and nitrogen fluxes (remobilisation and storage) occurring during the growth cycle of perennial plants such as *M. giganteus* (Fig. 1). The biomass of perennial organs, which correspond to the biomass of rhizomes and associated roots in the 0–25 cm soil depth, was distinguished from the biomass of non-perennial organs, which correspond to the biomass of shoots (Fig. 1a). In parallel, the nitrogen content of perennial organs was distinguished from the nitrogen content of non-perennial organs (Fig. 1b). The values of the principal parameters for the simulations are given in Table 1 with their definitions and units. Variables used in the equations added to the model are given in Table 2 with their definitions and units.

M. giganteus is able to remobilise part of the biomass and nitrogen included in its perennial organs [5, 12, 19, 23, 39]. The biomass and nitrogen content of perennial organs were divided into two compartments (Fig. 1 and Table 1): one compartment represents the biomass or the nitrogen reserves that can be remobilised by the plant (Eqs. 1 and 2) whilst the other represents the structural part of perennial organs and the reserves needed for their metabolism that cannot be remobilised by the plant (Eqs. 3 and 4). Neither direct biomass allocation to perennial organs nor direct nitrogen absorption occurs. Biomass and nitrogen dynamics in perennial organs are due to remobilisation and storage fluxes only (Fig. 1).

The model simulates the daily death of perennial organs (Eq. 5). Nitrogen losses from the death of perennial organs were calculated by multiplying the nitrogen concentration of perennial organs by their biomass (Eq. 6). Nitrogen or biomass remobilisations which could occur during the senescence of perennial organs were disregarded due to a lack of knowledge and a negligible impact on biomass and N fluxes.

In order to simulate the decrease in biomass during the senescence of vegetative aerial organs corresponding to stems plus leaves, temporary reserves located in the vegetative biomass of non-perennial above-ground organs were added (Fig. 1a). Temporary reserves are limited (Table 1), fixing the maximum proportion of biomass reserves that can be accumulated in the shoots. Temporary reserves evolve as a function of the proportion of living organs, represented by the evolution of the ratio between green leaf biomass and total leaf biomass (Eq. 7). The STICS model simulates leaf senescence and dead leaf drop [9]. Leaf senescence simulation is dynamic and occurs at the end of the leaf's lifespan. The dead leaf drop of *M. giganteus* occurs during the winter and not dynamically during the growing season [2]. We simulate dead leaf drop on a single date when the leaf area index is zero at the end of the growing season.

In parallel, the model simulates the evolution of the nitrogen content of vegetative aerial organs. Strullu et al. [39] showed that nitrogen accumulation in the vegetative organs ceased or drastically slowed down when leaf senescence began, corresponding to biomass storage starting in perennial organs. Hence, it was considered that nitrogen uptake by the plant is nil when biomass storage occurs. The structural nitrogen content of vegetative organs (Fig. 1b) is calculated daily by the model. Nitrogen fertilisation positively affects the nitrogen content of leaves and stems and results in a higher N content of senesced organs [37, 45, 46]. Dorsainvil [20] determined that the C/N ratio of *Sinapis alba* L. or *Lolium multiflorum* L. dead leaves evolves as a function of the plant's nitrogen nutrition index (Eq. 8). This concept was expanded to determine the evolution of dead stems C/N ratio (Eq. 9). The C/N ratio of dead leaves and stems depends on the plant parameters *Parazofmorte* and *Parazotmorte*, respectively (Table 1) (Eqs. 8 and 9) and on the plant's nitrogen nutrition index (NNI). The structural nitrogen content of vegetative organs is calculated daily by dividing the carbon biomass of vegetative organs by their C/N ratio (Eq. 10). Due to the important decrease of plant NNI during nitrogen storage, the model uses the NNI determined at the LAX stage, i.e. before N storage, in order to calculate the structural nitrogen content of the crop. The temporary nitrogen reserves of non-perennial organs, corresponding to metabolic nitrogen that can be remobilised by the crop, are calculated as the difference between nitrogen content in vegetative organs and their structural nitrogen content (Eq. 11).

Improvement of Biomass and Nitrogen Remobilisation Simulations

As previously defined by Brisson et al. [9], the remobilisation of biomass reserves from perennial organs to non-perennial organs occurs if daily assimilates are insufficient to satisfy the

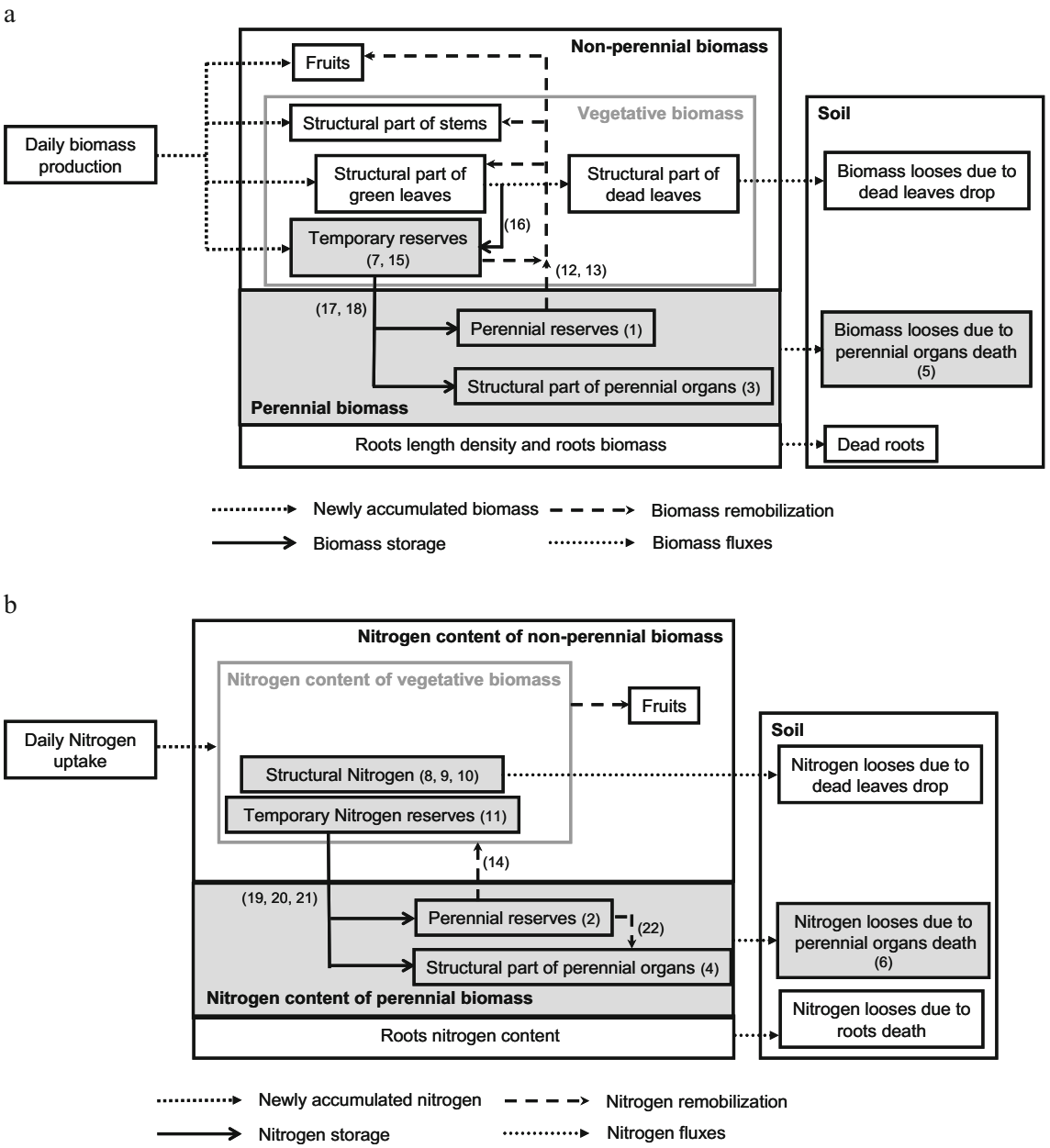

Fig. 1 Schematic representation of **a** biomass accumulation, partitioning and dynamic and **b** nitrogen accumulation, partitioning and dynamic. The *shaded areas* represent new pools simulated by the model. The *numbers in parenthesis* correspond to the equations added to the model for the simulation of new pools and fluxes

sink strength of vegetative and reproductive organs. This leads to the calculation of the first source/sink variable. Daily gross biomass remobilisation is restricted and stops if reserves are exhausted. In order to take into account the respiration of perennial organs associated to biomass and nitrogen remobilisation, the model calculation of a daily net biomass remobilisation was introduced. This flux is calculated by multiplying the daily gross biomass remobilisation by the plant's biomass remobilisation efficiency (Table 1) (Eq. 12). These remobilisations contribute to increasing the source/sink ratio the following day [9]. Some of the biomass reserves are lost in the form of CO_2 through respiration during remobilisation (Eq. 13).

It is considered that nitrogen remobilisation is linked and concomitant with biomass remobilisation. Daily nitrogen remobilisation is a function of nitrogen concentration in the reserve pool of perennial organs and of daily gross biomass remobilisation (Eq. 14). Moreover, plant nitrogen demand decreases during nitrogen remobilisation [9].

The accumulation of temporary reserves is due to two processes similar to those previously described for the perennial reserves [9]. Firstly, if daily assimilates exceed the plant's

Table 1 Definition and value of the principal parameters used for simulations

Parameters	Definition	Unit	Value	Sources
Propresp[a]	Proportion of biomass perennial reserves that can be remobilised	–	0.45	Strullu et al. [39]
ProprespN[a]	Proportion of nitrogen perennial reserves that can be remobilised	–	0.56	Strullu et al. [39]
Efremobil[a]	Remobilisation efficiency of perennial carbohydrates reserves	–	0.50	–
Propres[a]	Maximal proportion of biomass reserves in living vegetative organs	–	0.12	–
Tauxmortp[a]	Mortality rates of perennial organs	d^{-1}	0.001	–
CNrespstruc[a]	Minimum nitrogen concentration of structural compartment of perennial organs	%	3	Strullu et al. [39]
Parazofmorte	C/N ratio of dead leaves for a nitrogen nutrition index equal to 1	–	50	Strullu et al. [39]
Parazotmorte[a]	C/N ratio of dead stems for a nitrogen nutrition index equal to 1	–	260	Strullu et al. [39]
Efcroijuv	Maximum plant radiation use efficiency during juvenile growth	g DM MJ^{-1}	2.6	–
Efcroiveg	Maximum plant radiation use efficiency during vegetative growth	g DM MJ^{-1}	5.2	–
Efcroirepro	Maximum plant radiation use efficiency during reproductive growth	g DM MJ^{-1}	5.2	–
Temin	Minimum threshold temperature for net photosynthesis=base temperature	°C	6	Clifton-Brown et al. [13]
Teopt	Start of the thermal optimal plateau for net photosynthesis	°C	25	Beale et al. [4]
Teoptbis	End of the thermal optimal plateau for net photosynthesis	°C	30	–
Temax	Maximum threshold temperature for net photosynthesis	°C	40	Tuck et al. [44]
k	Plant extinction coefficient	–	0.70	Strullu et al. [40]
Dlaimaxbrut	Maximum leaf area index growth rate	m^2 $plant^{-1}$ dd^{-1}	0.018	Strullu et al. [40]
DurvieF	Maximum lifespan of an adult leaf	Q10	120	Strullu et al. [39]
Phyllotherme	Thermal time between emission of two consecutive leaves	dd	70	Pers. com. (O. Postaire)
Stlevamf	Thermal time duration between developmental stage lev (plant emergence) and stage amf (maximum acceleration of leaf area index development)	dd	300	Strullu et al. [40]
Stamflax	Thermal time duration between developmental stage amf and stage lax (end of emission of leaves)	dd	1,425	–
Stlevdrp	Thermal time duration between developmental stage lev and stage drp (start of grain filling)	dd	1,900	–
Stdrpflo	Thermal time duration between developmental stage drp and stage flo (flowering)	dd	0	–
adil	Parameter defining the critical nitrogen concentration when plant biomass is 1 t DM ha^{-1}	g kg^{-1}	3.0	–
bdil	Parameter defining the curvature of the nitrogen dilution curve	–	−0.47	–

[a] New parameters added to the model

structural biomass needs, then the surplus of assimilates is stored in the form of temporary reserves (Eq. 15). Secondly, part of the structural biomass is remobilised during leaf senescence and stored in the form of temporary reserves (Eq. 16). Therefore, it was necessary to deal with which of the two pools—perennial reserves or temporary reserves—had priority. The remobilisation of temporary reserves is calculated after the remobilisation of perennial reserves. Remobilisation occurs if the daily assimilates plus the remobilisation of perennial reserves is not sufficient to satisfy the sink strength of vegetative and reproductive organs [9]. This leads to the calculation of the second sources/sinks variable. Respiration associated with the remobilisation of temporary reserves is intrinsically taken into account by the model, which uses the plant's radiation use efficiency to simulate biomass production.

The transfer of biomass from temporary reserves to perennial organs was also dealt with. This occurs when the capacity of non-perennial vegetative organs to store biomass reserves is exceeded (Eq. 17). This biomass is first used to fill the compartment of remobilisable biomass. If the capacity to store the biomass of perennial organs is exceeded, the plant forms new perennial organs, allowing greater biomass storage in these latter (Eq. 18).

In contrast to the earlier version [9], the C and N relationship during remobilisation has been explained. Nitrogen transfer from non-perennial to perennial organs is linked to biomass transfer. The conditions for nitrogen transfer are different from those needed for biomass transfer. Firstly, if new perennial organs are formed, nitrogen is transferred to them in order to satisfy their nitrogen needs (Eq. 19). It is hypothesised that the nitrogen concentration of the structural part of perennial organs is stable (Table 1). Secondly, nitrogen storage in perennial organs occurs principally during the senescence of non-perennial vegetative organs, especially due to leaf senescence at the end of the plant's growth cycle. This occurs when there is no further appearance of new leaves i.e. the plant reaches the maximum leaf area index (development stage LAX). Daily nitrogen storage is then a function of the nitrogen concentration in the temporary reserves pool and of the daily biomass storage

Table 2 Definition and units of variables used in the equations presented in the Appendix

Variable	Definition	Equations	Units
Maperenne	Perennial organs biomass	1, 3, 5, 6, 18	t DM ha^{-1}
Resperenne	Perennial biomass reserves	1, 14, 18, 20, 21	t DM ha^{-1}
QNperenne	Nitrogen (N) content of the perennial organs	2, 4, 6	kg N ha^{-1}
QNresperenne	Perennial N reserves	2, 14	kg N ha^{-1}
Resperennestruc	Structural biomass pool of perennial organs	3	t DM ha^{-1}
QNresperennestruc	Structural N pool of perennial organs	4	kg N ha^{-1}
Δperennesen	Daily biomass losses due to perennial organs death	5, 6	t DM ha^{-1} d^{-1}
ΔQNperennesen	Daily N losses due to perennial organs death	6	kg N ha^{-1} d^{-1}
Masecveg	Biomass of non-perennial vegetative organs	7, 15	T DM ha^{-1}
Mafeuilverte	Biomass of the structural part of green leaves	7	t DM ha^{-1}
Mafeuil	Biomass of the structural part of leaves	7, 15	t DM ha^{-1}
Restempmax	Maximum temporary reserves that can be stored in living vegetative organs	7, 17, 20	t DM ha^{-1}
CsurNfeuil	C/N ratio of dead leaves	8	–
NNI	Nitrogen nutrition index of the plant	8, 9	–
CsurNtige	C/N ratio of dead stems	9	–
Cfeuil	Carbon biomass of the structural part of leaves	10	t C ha^{-1}
Ctigestruc	Carbon biomass of the structural part of stems	10	t C ha^{-1}
QNvegstruc	N content of the structural part of vegetative organs	10, 11	kg N ha^{-1}
QNveg	N content of the vegetative organs	11	kg N ha^{-1}
QNrestemp	Temporary N reserves located in living vegetative organs that can be remobilised by the plant	11, 20	kg N ha^{-1}
Δremobil	Daily net biomass remobilisation	12	t DM ha^{-1} d^{-1}
Δremobilbrut	Daily gross biomass remobilisation	12, 13, 14	t DM ha^{-1} d^{-1}
ΔCO2resperenne	Daily carbon losses due to perennial organs respiration	13	t C ha^{-1} d^{-1}
ΔremobilN	Daily N remobilisation from perennial organs	14	kg N ha^{-1} d^{-1}
Matigestruc	Biomass of the structural part of stems	15	t DM ha^{-1}
Restemp	Temporary reserves located in living vegetative organs	15, 17, 20	t DM ha^{-1}
Maenfruit	Dry matter of fruits envelopes	15	t DM ha^{-1}
ΔMS	Growth rate of the plant	16	t DM ha^{-1} d^{-1}
Δremobsen	Daily biomass remobilisation from senescing leaves to temporary reserves	16	t DM ha^{-1} d^{-1}
Pfeuilverte	Proportion of green leaves in non-perennial biomass	16	–
Δrestemp	Daily biomass storage from temporary reserves	17	t DM ha^{-1} d^{-1}
Alloresp	Allocation coefficient to perennial biomass reserves that can be remobilised by the plant	18	–
Δresper	Daily biomass storage from temporary reserves to perennial organs biomass reserves	18	t DM ha^{-1} d^{-1}
Δrespstruc	Daily biomass storage from temporary reserves to the structural biomass pool of perennial organs	18, 19, 21	t DM ha^{-1} d^{-1}
ΔrestempN	Daily N storage from temporary reserves to perennial organs	19, 20, 21	kg N ha^{-1} d^{-1}
ΔresperN	Daily N storage from temporary reserves to perennial organs N reserves	21, 22	kg N ha^{-1} d^{-1}
ΔrespstrucN	Daily N storage from temporary reserves to the structural N pool of perennial organs	21	kg N ha^{-1} d^{-1}
Resperennemax	Maximum perennial reserves that can be stored in perennial organs	21	t DM ha^{-1}
TransfN	Daily N transfer from perennial N reserves to the structural N pool of perennial organs	22	kg N ha^{-1} d^{-1}

flux (Eq. 20). Nitrogen allocation in perennial organs is a function of biomass partitioning and maintaining a stable nitrogen concentration in their structural part (Eq. 21). If the daily nitrogen transfer flux is not sufficient to satisfy the nitrogen needs of the structural part of perennial organs, there is a nitrogen transfer from the remobilisable nitrogen pool of perennial organs to the structural nitrogen pool of perennial organs (Eq. 22).

Model Calibration and Evaluation

Field Experiment

Experimental data has come from field experiments in the Picardie region of northern France (49° 52′ N, 3° 00′ E). Biomass production and the environmental impacts of different cropping systems dedicated to bioenergy production were

studied in this experiment [11, 39]. *M. giganteus* was planted in May 2006. Different treatments have been applied to *M. giganteus* cropping systems since 2007 in terms of harvest date (EH=early harvest in October of the green up year and LH=late harvest in February/March of the next year after green up) and nitrogen fertilisation rate (N0=0 and N1=120 kg N ha^{-1} y^{-1}). Details on emergence date, harvest date, nitrogen fertiliser rates and harvested biomass from 2008 to 2012 with the different treatments are given in Table 3. The experimental data of late harvest treatments (LHN0 and LHN1) for the 2008–2009 growing season were used for model calibration. The experimental data from early harvest treatments (EHN0 and EHN1) from 2008 to October 2011 and the experimental data from late harvest treatments from 2009 to March 2012 were used for model validation.

Statistical Analysis

The model performance was characterised by calculating various complementary statistical criteria based on the comparison of observed and simulated data. This allowed the quality of model simulations to be quantified by estimating the magnitude of the model error, the dominant type of the model error (bias or dispersion) and the capacity to reproduce observed data variability for each output variable.

The model error (model residual) was estimated by the root mean square error (RMSE), which has the same unity as the variable:

$$RMSE = \sqrt{\frac{1}{n}\cdot\sum_{i=1}^{n}(P_i - O_i)^2} \quad (25)$$

with O and P the observed and predicted values, respectively and n the number of observed-estimated pairs. The lower the values, the better the model prediction. The *RMSE* was then split into two components describing the systematic error ('bias' *RMSEs*) and the unsystematic error ('dispersion' *RMSEu*), calculated as follows [48]:

$$RMSEs = \sqrt{\frac{1}{n}\cdot\sum_{i=1}^{n}\left(\widehat{P}_i - O_i\right)^2} \quad (26)$$

$$RMSEu = \sqrt{\frac{1}{n}\cdot\sum_{i=1}^{n}\left(P_i - \widehat{P}_i\right)^2} \quad (27)$$

with $\widehat{P}_i$ derived from the linear regression of predicted versus observed values: $\widehat{P}_i = a + b{\cdot}O_i$ and a and b the parameters of the regression. The element of variance attributable to systematic error (*pRMSEs* in %) was calculated by:

$$pRMSEs = 100\cdot\frac{RMSEs^2}{RMSE^2} \quad (28)$$

Two widely used statistical criteria were calculated to determine the model's performance: modelling efficiency (*EF*) and the coefficient of determination (R^2). R^2 is the square of Pearson's correlation coefficient of estimates versus measurements and describes the proportion of the

Table 3 *Miscanthus*× *giganteus* above-ground biomass yields± standard error (t DM ha^{-1}) measured over 4 years of growth and subject to different cultural practices

Treatment	Emergence date	Harvest date	Fertiliser inputs (kg N ha^{-1})	Measured yield (t DM ha^{-1})
LHN0	01/04/2008	05/03/2009	0	19.1±1.7
	07/04/2009	04/03/2010	0	20.9±2.0
	24/04/2010	03/03/2011	0	22.2±2.2
	08/04/2011	13/03/2012	0	20.9±2.5
LHN1	01/04/2008	05/03/2009	120	19.5±2.3
	07/04/2009	04/03/2010	120	20.6±1.9
	24/04/2010	03/03/2011	120	22.0±2.9
	08/04/2011	13/03/2012	120	19.5±1.9
EHN0	01/04/2008	20/10/2008	0	24.0±2.6
	03/04/2009	12/10/2009	0	24.0±3.3
	12/04/2010	12/10/2010	0	26.1±1.5
	28/03/2011	26/10/2011	0	16.1±0.9
EHN1	01/04/2008	20/10/2008	120	26.6±3.3
	03/04/2009	12/10/2009	120	27.7±0.9
	12/04/2010	12/10/2010	120	28.5±0.2
	28/03/2011	26/10/2011	120	26.9±1.1

LHN0 late harvest in February/March of the next year after green up without nitrogen fertilisation, *LHN1* late harvest in February/March of the next year after green up with nitrogen fertilisation, *EHN0* early harvest in October of the green up year without nitrogen fertilisation, *EHN1* early harvest in October of the green up year with nitrogen fertilisation

total variance in the observed data that can be explained by the model:

$$R^2 = \left[\frac{\sum_{i=1}^{n}\left(P_i-\overline{P}\right)\cdot\left(O_i-\overline{O}\right)}{\sigma_{EP}\cdot\sigma_O}\right] \quad (29)$$

with $\overline{P}$ and $\overline{O}$ the mean of estimated and observed values, respectively. R^2 characterises the ability to account for the dispersion, but does not account for any systematic error (i.e. bias).

EF is a measure of agreement between estimates and observations, calculated as follows:

$$EF = 1-\frac{\sum_{i=1}^{n}(P_i-O_i)^2}{\sum_{i=1}^{n}\left(O_i-\overline{O}\right)} \quad (30)$$

It varies from 1 (best performance) to an infinite negative value, with a negative value indicating that the mean of observations is a better predictor than the model.

Results

Leaf Area Index

The model accurately simulates the leaf area index (LAI) dynamic and reproduces rapid LAI growth until mid-August (Fig. 2). However, maximum LAI was overestimated during the growing season 2009–2010. LAI decreases during autumn due to leaf senescence which is also simulated effectively by the model. An acceleration of leaf senescence is simulated when water stress or frost occurred during the growing season. The statistical analysis revealed that the model satisfactorily simulates the leaf area index of the plant with different treatments and during different years of growth with an R^2 of 0.74 and a model efficiency of 0.46 (Table 4). There was high variability in the simulations, with an RMSE of 1.6 m^2 m^{-2} for the validation set.

Biomass Production and Partitioning in the Crop

The model accurately simulates the plant's total biomass (Fig. 3). It reproduces the biomass dynamic in perennial organs, with a phase of biomass remobilisation from emergence until the end of spring, followed by a phase of biomass storage until total senescence of shoots. The model was also able to simulate accurately the biomass of plant shoots and the decrease in the shoots' dry matter due to biomass storage and leaf drop during the autumn and winter. The statistical analysis revealed that the model correctly simulates the plant's total and above-ground biomass in different treatments and during different years of growth with an R^2 and model efficiency of 0.93 and 0.95, respectively (Table 4). The model simulates less well, but nevertheless satisfactorily, the biomass of perennial organs, with an R^2 of 0.58 and a model efficiency of 0.41 (Table 4).

Biomass partitioning between stems, green leaves and dead leaves is correctly reproduced by the model despite the fact that a formal comparison is impossible since the model does not allocate metabolic reserves but only structural ones (Fig. 4). The model simulates the structural biomass of stems and a preferential allocation of temporary biomass reserves to them, leading to an expected underestimation of the biomass of stems (Fig. 4) and a high systematic error (Table 4). The statistical analysis revealed that the model accurately simulates stem, green leaf and dead leaf biomass with a high R^2 (0.84 to 0.97) and high model efficiency (0.79 to 0.95) (Table 4).

Nitrogen Uptake and Nitrogen Dynamics in the Crop

The model accurately simulates nitrogen dynamics in perennial organs, notably the nitrogen remobilisation to shoots during spring regrowth (Fig. 5). With regard to nitrogen dynamics in shoots, the model reproduces the rapid nitrogen accumulation until July and then plateaus. The model then simulates a rapid decrease in the nitrogen content of shoots from mid-September until leaves drop at the beginning of December (Fig. 5). The nitrogen content of the entire plant is simulated effectively, with a period of nitrogen accumulation until July which then plateaus until the leaves drop. The plant's nitrogen content and its partitioning between perennial and non-perennial organs are validated by the statistical analysis with an R^2 and model efficiency included between 0.63 and 0.75 (Table 4).

Simulations of the Effect of Cultural Practices on Biomass Production and Nitrogen Accumulation

Results of simulations over 4 years of growth for early harvest treatment without nitrogen fertilisation (EHN0) are presented in Fig. 6. The plant's biomass production in shoots was slightly overestimated in 2008. Thereafter biomass production in shoots is accurately simulated by the model, notably the decrease of biomass in shoots observed in 2011 (Fig. 6a). The biomass dynamic of perennial organs and the total biomass of the plant are also correctly simulated by the model (Fig. 6a).

With regard to shoots and total plant nitrogen content, the model overestimates the nitrogen uptake, particularly in 2008 (Fig. 6b). The model accurately reproduces the nitrogen dynamic in the crop, notably the decrease of perennial nitrogen stocks observed in 2010. The model is able to reproduce the

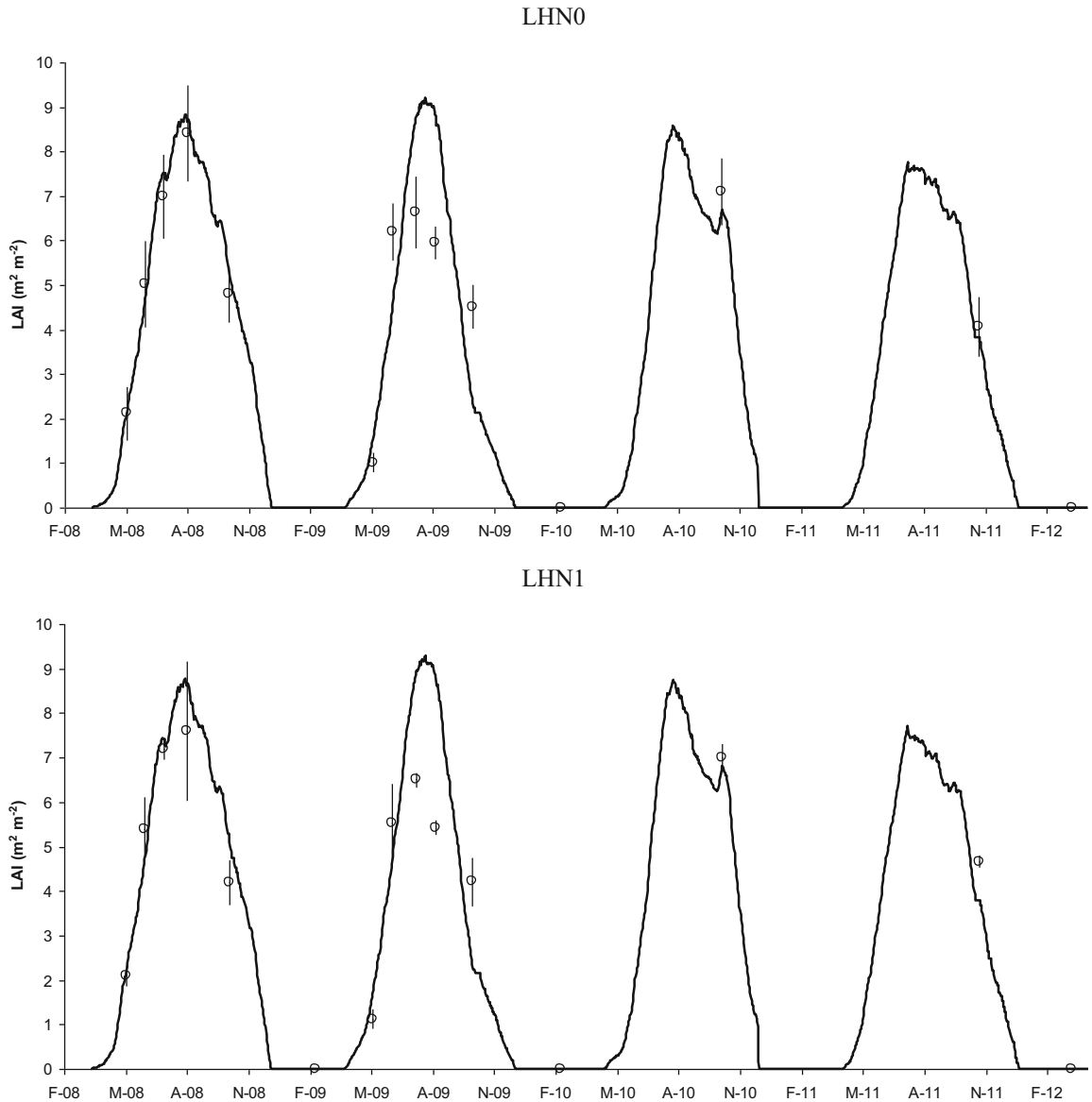

Fig. 2 Leaf area index (*LAI*) simulated by the model for late harvest treatment with (*LHN1*) or without (*LHN0*) nitrogen fertilisation during four growing seasons. The first growing season corresponds to the calibration of the model. *Open black diamonds* LAI-observed data, *black line* LAI-simulated data

effect of the harvest date on nitrogen exports and the evolution of nitrogen stocks in perennial organs due to harvest before the plant's total senescence (Fig. 6b).

The statistical analysis revealed that the model correctly simulates the effect of management practices on plant's harvest yield with an R^2 and model efficiency of 0.68 and 0.70, respectively (Table 4). The model simulates that N fertilisation had no effect on late harvest treatments yields as observed in the field. Observed yields of LHN1 treatment relative to LHN0 treatment were 102, 99, 99 and 93 % for the 4 years (Table 3) and simulated yields were 99, 102, 103 and 98 %. Moreover, the model was able to reproduce the positive effect of N fertilisation on early harvest treatments yields. Observed yields of EHN1 treatment relative to EHN0 treatment were 111, 115, 109 and 167 % for the 4 years (Table 3) and simulated yields were 99, 102, 112 and 128 %. Finally, the model successfully simulated the effect of harvest date: observed yields of LH treatments relative to EH treatments were 76, 80, 81 and 94 % in average for the 4 years (Table 3) and simulated yields were 75, 86, 80 and 98 %.

Discussion

Leaf Area Index and Dead Leaves Drop

The plant's leaf area index development (LAI) and radiation use efficiency (RUE) are key physiological processes for

Table 4 Model evaluation statistics of plant attributes for the validation set

Plant validation set	*N*	*X* obs	*X* sim	R^2	RMSE	pRMSEs	pRMSEu	EF
Leaf area index	42	4.3	4.6	0.74	1.6	0.88	0.12	0.46
Total plant biomass	38	29.8	29.7	0.93	3.2	0.04	0.96	0.93
Shoot biomass	44	19.3	19.7	0.95	2.1	0.17	0.83	0.95
Perennial organ biomass	38	14.4	13.6	0.58	3.0	0.10	0.90	0.41
Stem biomass	44	15.5	14.9	0.97	1.7	0.50	0.50	0.95
Green leaf biomass	44	2.7	2.4	0.84	0.7	0.13	0.87	0.79
Dead leaf biomass	44	1.1	1.0	0.93	0.3	0.19	0.81	0.92
Total plant N content	38	249.4	247.5	0.75	41.9	0.11	0.89	0.75
Shoot N content	44	130.2	127.4	0.75	33.4	0.01	0.99	0.70
Perennial organ N content	38	138.6	133.8	0.71	34.2	0.02	0.98	0.63
Harvest yield	14	23.3	23.1	0.68	1.9	0.27	0.73	0.70

N number of measured/simulated data pairs, *Xobs* mean of measured values, *Xsim* mean of simulated values, R^2 coefficient of determination of the linear regression between simulated and measured values, *RMSE* root mean squared error, *pRMSEs* part of variance attributable to the systematic error ('bias'), *pRMSEu* part of variance attributable to the unsystematic error ('dispersion'), *EF* model simulation efficiency

simulating the plant's biomass production. The LAI dynamic of *M. giganteus* during the growing season was accurately simulated by the model. However, it was observed that the model overestimated LAI growth and leaf senescence when there was water stress (year 2009 Fig. 2). This led to an overestimation of the maximum LAI attained by the plant and a faster decrease in LAI at the end of the 2009–2010 growing season. These overestimations do not have a significant impact on the simulations of biomass production in the plant because the LAI observed in experimental conditions was not a limiting factor for the interception of radiation [40]. It can also indirectly influence the biomass of senescent leaves. Therefore, some improvements will be needed in order to create better LAI simulations in dryer environments where LAI development and the maximum LAI reached by the plant could be limiting factors for plant biomass production, as observed by Cosentino et al. [15].

We simulated a sudden dead leaf drop when the LAI becomes zero at the end of the growing season. In fact, dead leaf drop occurs during winter after total senescence of the plant [2], depending on climate conditions. However this simplification (sudden fall) has a very limited impact on residue decomposition dynamics due to the constant presence of a mulch at soil surface characterised by a slow decomposition rate, according to Amougou et al. [2].

Biomass Production and Partitioning

The maximum achievable total RUE was calibrated at 5.2 g MJ^{-1} of intercepted photosynthetic active radiation (Table 1). This value is higher than the maximum RUE observed of 4.1 g MJ^{-1} for sugarcane [38], a C4 plant of the same family than *M. giganteus*, or than the mean maximum RUE observed of 4.7 g MJ^{-1} for switchgrass, a perennial C4 grass, in optimal environmental conditions [28]. However, these latter values did not take into account the C allocation to the belowground organs of the crop. The range of RUE values reported in the literature for *M. giganteus* vary between 1.1 and 4.1 g MJ^{-1} [4, 14, 15, 26, 40, 41], with a high variability which is due to different ages of the plantations [40], various climatic conditions and differences in methodology between studies. Again, these values are relative to aerial parts and did not include the belowground organs. Hence, the maximum RUE found for the above-ground biomass (4.1 g MJ^{-1}) has to be raised to account for the accumulation of biomass in belowground organs, occurring between the end of the remobilisation phase (early July) and the beginning of the remobilisation of aerial reserves towards rhizomes (end of September). In our previous study [39, 40], the mean observed RUE for aerial parts was 3.43 g MJ^{-1} for a biomass production of 23.9 t ha^{-1} and the net biomass accumulation in belowground organs was 8.5 t ha^{-1}. Assuming a similar conversion efficiency, the RUE of belowground organs would be $3.43 \times 8.5/23.9 = 1.22$ g MJ^{-1}, yielding a total RUE of 4.65 g MJ^{-1}. Hence, it appears that the maximum total RUE of 5.2 g MJ^{-1} is realistic. This high conversion efficiency of photosynthate to biomass found in *M. giganteus* is attributed to its high content in cellulose and starch and its very low content in proteins and lipids [16]. Jing et al. [25] used a higher value of total RUE (5.97 g MJ^{-1}) but their model does not account for biomass remobilisation from perennial to non-perennial organs.

Certain apparent paradoxes in this conceptualisation can be explained by only taking respiration into account in upward remobilisation as opposed to a downward one. In the latter, respiration is included in the system that allows the RUE calculation, because the respired carbohydrates are located in aerial dry matter. Conversely, respiration during upward

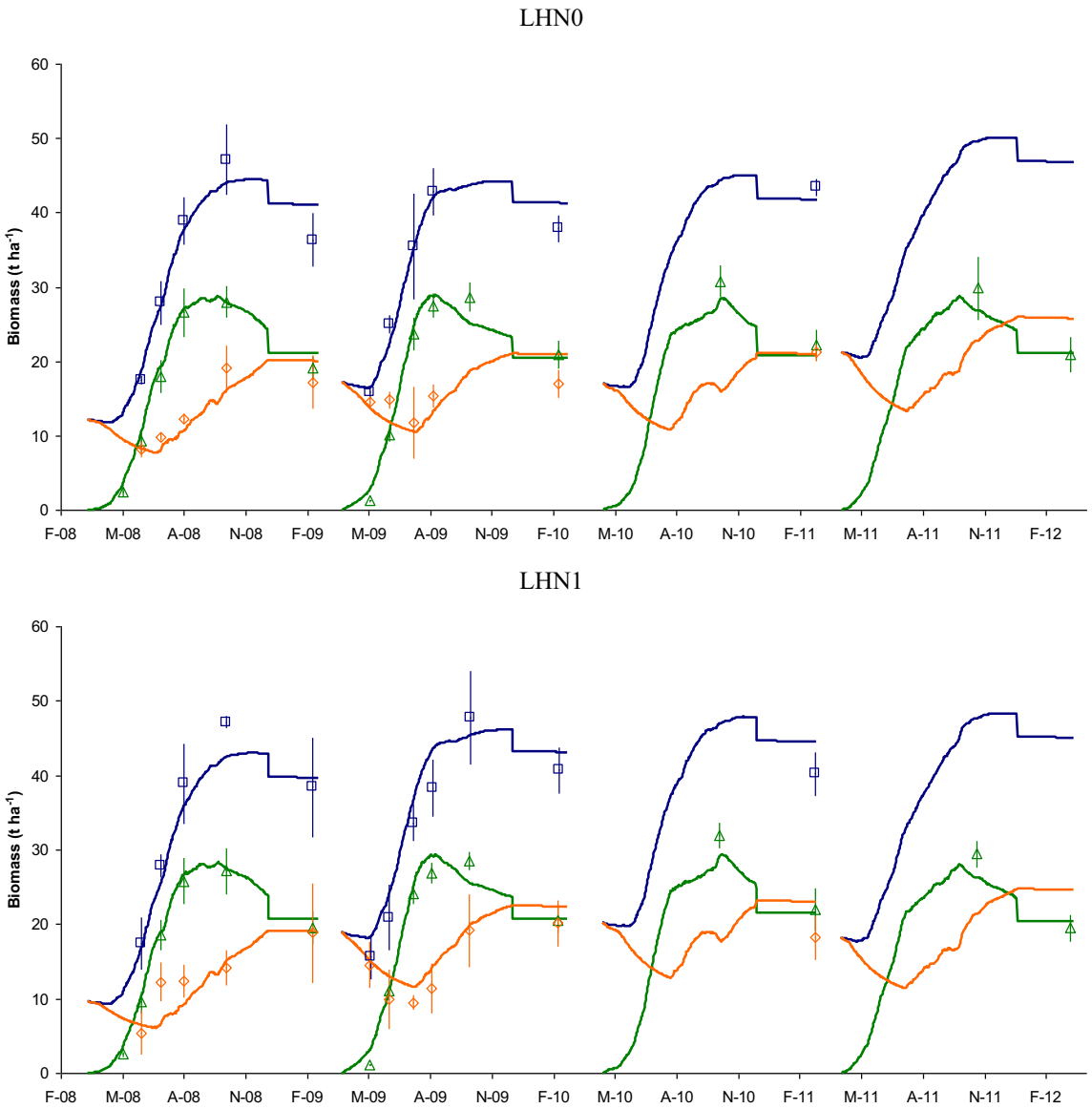

Fig. 3 Biomass accumulation and dynamic simulated by the model during four growing seasons. The first growing season corresponds to the calibration of the model. *LHN1* late harvest treatment with nitrogen fertilisation, *LHN0* late harvest treatment without nitrogen fertilisation. *Open orange diamonds* observed data for belowground organs, *open green triangles* observed data for above-ground organs, *open blue squares* observed data for whole plant. *Orange line* simulated data for belowground biomass, *green line* simulated data for above-ground biomass, *blue line* simulated data for whole plant biomass

remobilisation is located in the rhizomes which do not belong to the system allowing the RUE calculation.

The capacity of the model to simulate accurately biomass production in shoots and partitioning in the structural parts of stems and leaves allows an accurate simulation of biomass allocation to the reserves pools. De Souza et al. [16] showed that temporary biomass reserves were predominantly found in *M. giganteus* stems, confirming biomass partitioning simulated by the model. This resulted in a realistic simulation of the reserves dynamic in the crop, confirmed by the model's accuracy at simulating shoots and the biomass of perennial organs. The dynamic of perennial organs, with a decrease from plant emergence to the end of June followed by an increase in the biomass of perennial organs due to biomass storage, is consistent with other studies [5, 23]. Thanks to modifications made to the model, it is now able to simulate the effect of harvest dates on *M. giganteus* shoots and the biomass of perennial organs.

Nitrogen Accumulation and Partitioning

As far as is known, there is only one model which takes into account nitrogen remobilisation during perennial plant regrowth [25]. It should be noted that regrowth in perennial

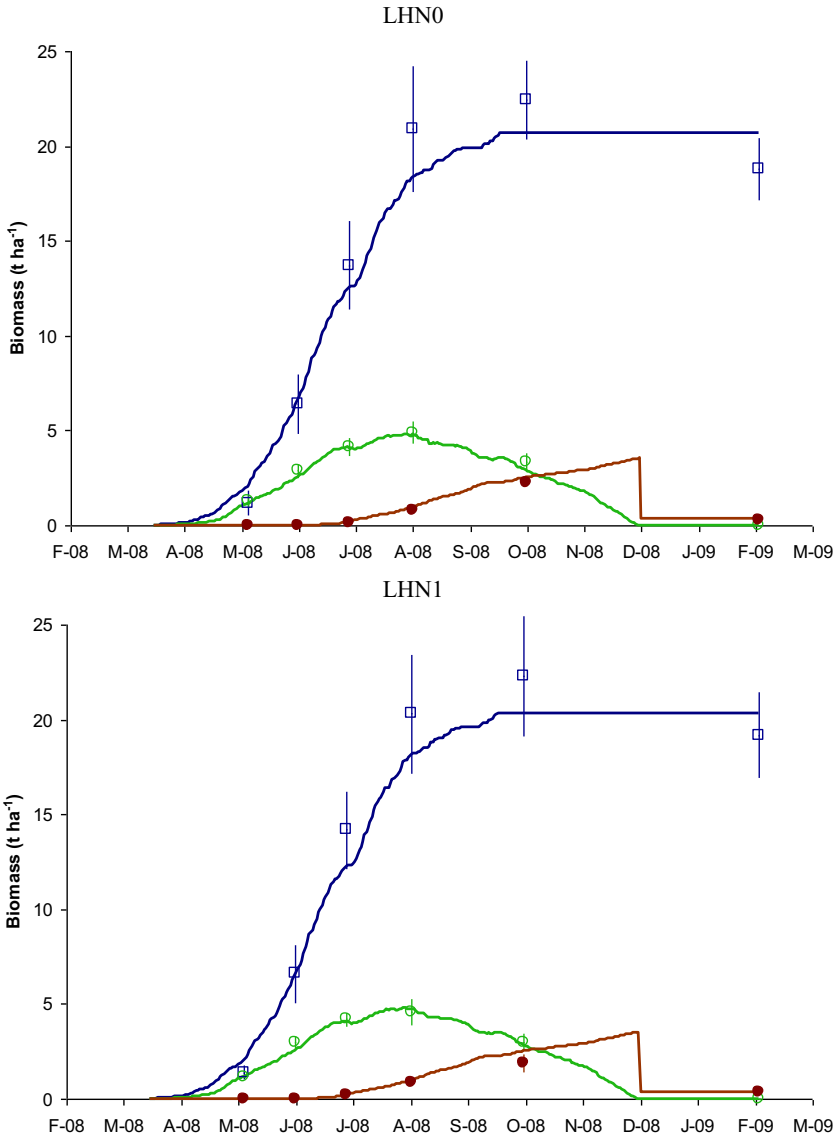

Fig. 4 Vegetative organs biomass simulated by the model during the first growing season (model calibration). *LHN1* late harvest treatment with nitrogen fertilisation, *LHN0* late harvest treatment without nitrogen fertilisation. *Open blue squares* observed data for stems biomass, *open green circles* observed data for green leaves biomass, *solid brown circles* observed data for dead leaf biomass. *Blue line* simulated data for structural biomass of stems, *green line* simulated data for structural biomass of green leaves, *brown line* simulated data for dead leaves biomass

grasses is heavily dependent on the nitrogen stocks available after cutting. However, this model is not able to simulate nitrogen storage. It is essential to take nitrogen remobilisation and storage into account in order to simulate *M. giganteus* biomass production and nitrogen fertiliser requirements [39, 40]. Thanks to the modifications made to the STICS model, simulation of these fluxes is now feasible.

The critical nitrogen dilution curve for *M. giganteus* was calibrated with data used for model calibration and validation (Table 1). Lower parameter values were found for the critical nitrogen dilution curve of *M. giganteus* than those determined for other C4 crops, such as maize or sorghum [21, 35]. This result is in line with the study by Cadoux et al. [10] who explained that the nitrogen requirements of *M. giganteus* are lower than those of *Zea mays*.

Nitrogen remobilisation simulated by the model, with a decrease in belowground nitrogen stocks from plant emergence until mid-July, is in line with other studies [5, 23]. In this model, nitrogen uptake is considerably limited or stops altogether during nitrogen remobilisation and nitrogen storage. Different authors have shown that nitrogen uptake is inhibited during nitrogen remobilisation [24, 34, 43]. The STICS model already took into account the decrease of nitrogen uptake in the spring during nitrogen remobilisation from perennial organs to shoots or during nitrogen remobilisation from shoots to reproductive organs [7]. This concept has been expanded to internal nitrogen remobilisation from senescent leaves to growing leaves which occurred during *M. giganteus* growth. It is considered that nitrogen uptake by the plant stopped during those remobilisations, which allowed the simulation of the plateau in plant nitrogen content observed in different field experiments [5, 19, 23, 39]. The model also reproduced the absence of nitrogen uptake at the beginning of *M. giganteus* regrowth from emergence until May [23]. The

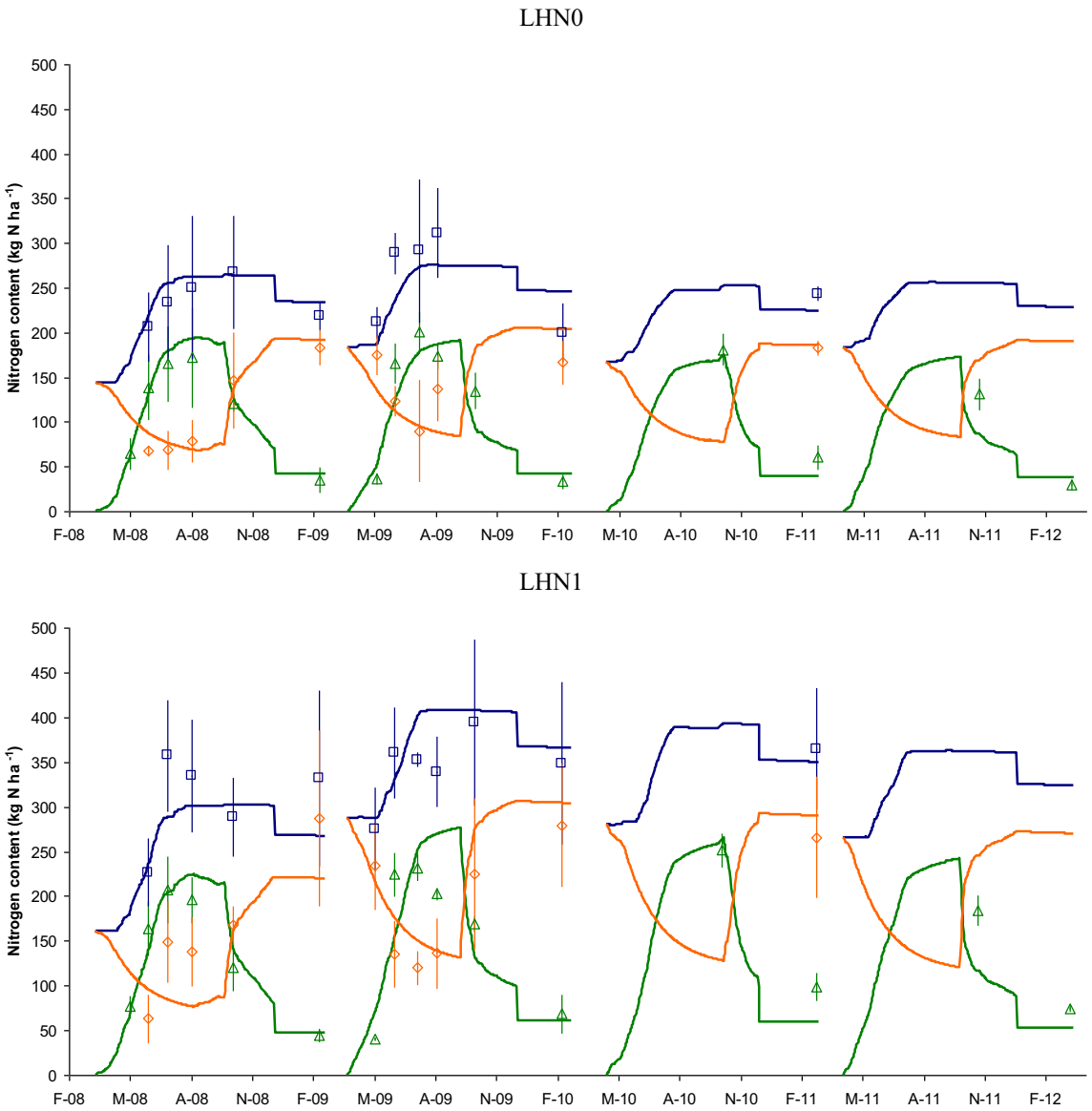

Fig. 5 Nitrogen uptake and dynamic in the plant simulated by the model during four growing seasons. The first growing season corresponds to the calibration of the model. *LHN1* late harvest treatment with nitrogen fertilisation, *LHN0* late harvest treatment without nitrogen fertilisation. *Open orange diamonds* observed data for belowground organs, *open green triangles* observed data for above-ground organs, *open blue squares* observed data for whole plant. *Orange line* simulated data for belowground organs, *green line* simulated data for above-ground organs, *blue line* simulated data for whole plant

rapid nitrogen storage simulated by the model from the end of September to total senescence in December is in line with the study by Himken et al. [23] and the review by Cadoux et al. [10]. Thanks to modifications made to the STICS model, the effect of harvest date and nitrogen fertilisation on nitrogen export from the field at harvest and on the evolution of the nitrogen content of perennial organs can now be simulated.

Required Improvements to the Soil Sub-Model

Surprisingly, despite the end of the plant's nitrogen uptake in summer, the soil's mineral nitrogen content in November is low in the *M. giganteus* cropping system [39]. The model simulated the end of nitrogen uptake by *M. giganteus* effectively, but it led to an overestimation of the soil's mineral nitrogen content at the end of the growing season (data not shown). Although the death of roots and perennial organs is simulated dynamically (Fig. 1), decomposition only starts on the harvest date. In order to simulate the soil's mineral nitrogen content accurately, the daily decomposition of dead roots and dead perennial organs must be added to the model. Decomposition of the dead organs of *M. giganteus* leads to a net immobilisation of

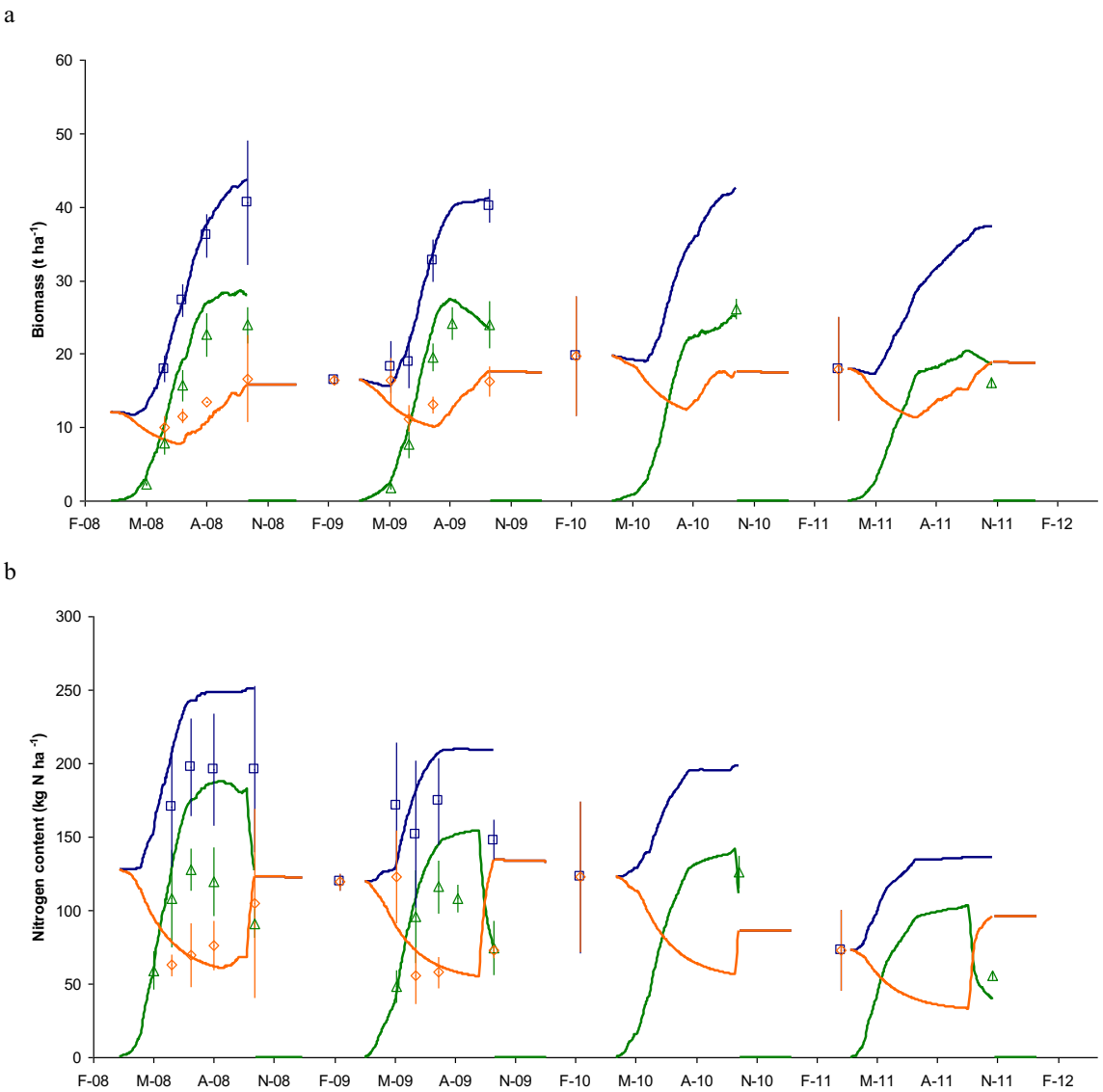

Fig. 6 Model evaluation in early harvest treatment without nitrogen fertilisation (EHN0) for **a** biomass content and **b** nitrogen content of *Miscanthus*×*giganteus*. *Open orange diamonds* observed data for belowground organs, *open green triangles* observed data for above-ground organs, *open blue squares* observed data for whole plant. *Orange line* simulated data for belowground biomass, *green line* simulated data for above-ground biomass, blue line simulated data for whole plant biomass

nitrogen in the soil [1]. Daily decomposition of dead leaves is already simulated by the model [9]. With these modifications, the model should be able to simulate the evolution of the soil's nitrogen supply during the growing season and the soil's mineral nitrogen content at the end of the growing season and hence improve the quality of simulations for N uptake and biomass production by the plant.

It is important to state that the simulation of nitrogen dynamics in the plant is very sensitive to the emergence date. Indeed, nitrogen storage occurred very quickly at the end of the growing season during plant senescence. Observed data was used to start the simulations in this study. Model parameterisation and calibration for an accurate simulation of plant dormancy and emergence will be necessary to link simulations together over the long term.

In this study, the model was tested in just one pedoclimatic environment. The objectives of this study were to present new equations added to the plant model STICS in order to simulate biomass and nitrogen dynamic in the perennial organs and shoots of *M. giganteus* and to demonstrate its ability to simulate the effect of cultural practices on the plant's biomass and nitrogen content. It will soon be used to simulate the plant's biomass production and environmental impacts in contrasting pedoclimatic environments in order to test its robustness.

Conclusions

As far as it is possible to ascertain, this new version of the STICS model is the first to simulate biomass and nitrogen dynamics in perennial and non-perennial organs. It has been shown that the model is able to simulate accurately the biomass and nitrogen dynamics in the shoots and perennial organs of *M. giganteus*. During this study, care was taken to develop a generic model allowing the simulation of biomass and nitrogen partitioning between structural and metabolic pools in perennial and non-perennial organs. The parameterisation and calibration of the model for other plants (annual or perennial plants) in order to produce better simulations of their biomass production and environmental impacts is therefore possible. In future, the STICS model will be used to evaluate the biomass production and environmental impacts of *M. giganteus* over the long term in different pedoclimatic conditions. Moreover, it could be used to support research into the ideotype of perennial plants dedicated to bioenergy production. Indeed, this process-based model will allow an investigation into the effect of changes in cultural practices and physiological parameters on biomass production and environmental impacts of the plant.

Acknowledgments The assistance provided by C. Demay, C. Dominiarczyk, J. Haxaire, E. Mignot, M. Preudhomme and A. Teixeira and the experimental unit around the acquisition of data is gratefully acknowledged. The authors gratefully thank M. Launay for the time spent for constructive discussions on the model. The authors thank all physiologists and modellers around the world whose work and publications allow the modelling of plant processes. This research has been funded by OSEO as part of the Futurol project.

Appendix: Model Equations

1. Perennial organs (Rhizome and associated coarse roots in 0–25 cm depth)

Remobilisable biomass and nitrogen

$$\mathrm{RESPERENNE} = \mathrm{PROPRESP} \times \mathrm{MAPERENNE} \quad (1)$$

$$\mathrm{QNRESPERENNE} = \mathrm{PROPRESPN} \times \mathrm{QNPERENNE} \quad (2)$$

Non remobilisable biomass and nitrogen

$$\mathrm{RESPERENNESTRUC} = (1 - \mathrm{PROPRESP}) \times \mathrm{MAPERENNE} \quad (3)$$

$$\mathrm{QNRESPERENNESTRUC} = (1 - \mathrm{PROPRESPN}) \times \mathrm{QNPERENNE} \quad (4)$$

Death

$$\Delta\mathrm{PERENNESEN} = \mathrm{TAUXMORTP} \times \mathrm{MAPERENNE} \quad (5)$$

$$\Delta\mathrm{QNPERENNESEN} = \Delta\mathrm{PERENNESEN} \times \frac{\mathrm{QNPERENNE}}{\mathrm{MAPERENNE}} \quad (6)$$

2. Non-perennial organs (stems and leaves)

Maximal temporary reserves

$$\mathrm{RESTEMPMAX} = \mathrm{PROPRES} \times \frac{\mathrm{MAFEUILVERTE}}{\mathrm{MAFEUIL}} \times \mathrm{MASECVEG} \quad (7)$$

C/N ratio and nitrogen contents

$$\mathrm{CSURNFEUIL} = \frac{\mathrm{PARAZOFMORTE}}{\mathrm{NNI}} \quad (8)$$

$$\mathrm{CSURNTIGE} = \frac{\mathrm{PARAZOTMORTE}}{\mathrm{NNI}} \quad (9)$$

$$\mathrm{QNVEGSTRUC} = \left[\frac{\mathrm{CFEUIL}}{\mathrm{CSURNFEUIL}}\right] + \left[\frac{\mathrm{CTIGESTRUC}}{\mathrm{CSURNTIGE}}\right] \quad (10)$$

$$\mathrm{QNRESTEMP} = \mathrm{QNVEG} - \mathrm{QNVEGSTRUC} \quad (11)$$

Biomass and nitrogen remobilisation

$$\Delta\text{REMOBIL} = \text{EFREMOBIL} \times \Delta\text{REMOBILBRUT} \quad (12)$$

$$\Delta CO2\text{RESPERENNE} = 0.40 \times (1 - \text{EFREMOBIL}) \times \Delta\text{REMOBILBRUT} \quad (13)$$

$$\Delta\text{REMOBILN} = \Delta\text{REMOBILBRUT} \times \frac{\text{QNRESPERENNE}}{\text{RESPERENNE}} \quad (14)$$

Temporary reserves

$$\text{RESTEMP} = \text{MASECVEG} - \text{MAFEUIL} - \text{MATIGESTRUC} - \text{MAENFRUIT} \quad (15)$$

$$\Delta\text{REMOBSEN} = \sum_{J=1}^{n} \Delta\text{MS}(J) \cdot (1-\text{RATIOSEN}) \cdot \text{PFEUILVERTE}(J) \quad (16)$$

with n=leaf lifespan

3. Transfer and allocation

Biomass transfer and its allocation:

$$\Delta\text{RESTEMP} = \text{RESTEMP} - \text{RESTEMPMAX} \quad (17)$$

```
if      RESPERENNE < PROPRESP × MAPERENNE  then
        ΔRESPER  = ΔRESTEMP
        ΔRESPSTRUC  = 0
else
        ΔRESPER  = PROPRESP  × ΔRESTEMP
        ΔRESPSTRUC  = (1 − PROPRESP) × ΔRESTEMP
endif
```

(18)

Nitrogen transfer and its allocation:

$$\Delta\text{RESTEMPN} = \Delta\text{RESPSTRUC} \times \text{CNRESPSTRUC} \quad (19)$$

$$\Delta\text{RESTEMPN} = \Delta\text{RESTEMP} \times \frac{\text{QNRESTEMP}}{\text{RESTEMP}} \quad (20)$$

```
if      RESPERENNE < RESPERENNEMAX  then
        ΔRESPSTRUCN  =  0
        ΔRESPERN = ΔRESTEMPN
else
        ΔRESPSTRUCN = ΔRESPSTRUC × CNRESPSTRUC
        ΔRESPERN  =  ΔRESTEMPN  −  ΔRESPSTRUCN
endif
```

(21)

$$\text{if} \quad \Delta\text{RESPERN} < 0 \quad \text{then} \quad \text{TRANSFN} = -\Delta\text{RESPERN} \quad (22)$$

References

1. Amougou N, Bertrand I, Machet JM, Recous S (2011) Quality and decomposition in soil of rhizome, root and senescent leaf from *Miscanthus x giganteus*, as affected by harvest date and N fertilization. Plant Soil 338:83–97
2. Amougou N, Bertrand I, Cadoux S, Recous S (2012) *Miscanthus x giganteus* leaf senescence, decomposition and C and N inputs to soil. GCB Bioenergy 4:698–707
3. Avice JC, Lemaire G, Ourry A, Boucaud J (1997) Effects of the previous shoot removal frequency on subsequent shoot regrowth in two *Medicago sativa L*. cultivars. Plant Soil 188:189–198
4. Beale CV, Long SP (1995) Can perennial C4 grasses attain high efficiencies of radiant energy conversion in cool climates? Plant Cell Environ 18:641–650
5. Beale CV, Long SP (1997) Seasonal dynamics of nutrient accumulation and partitioning in the perennial C4-grasses *Miscanthus x giganteus* and *Spartina cynosuroides*. Biomass Bioenergy 12:419–428
6. Beaudoin N, Launay M, Sauboua E, Ponsardin G, Mary B (2008) Evaluation of the soil plant model STICS over 8 years against the "on farm" database of Bruyères catchment. Eur J Agron 29:46–57
7. Brisson N, Mary B, Ripoche D, Jeuffroy MH, Ruget F, Nicoullaud B, Gate P, Devienne-Barret F, Antonioletti R, Durr C, Richard G, Beaudoin N, Recous S, Tayot X, Plenet D, Cellier P, Machet JM, Meynard JM, Delécolle R (1998) STICS: a generic model for the simulation of crops and their water and nitrogen balances. I Theory and parameterization applied to wheat and corn. Agronomie 18:311–346
8. Brisson N, Gary C, Justes E, Roche R, Mary B, Ripoche D, Zimmer D, Sierra J, Bertuzzi P, Burger P, Bussière F, Cabidoche YM, Cellier P, Debaeke P, Gaudillère JP, Hénault C, Maraux F, Seguin B, Sinoquet H (2003) An overview of the plant model STICS. Eur J Agron 18:309–332
9. Brisson N, Launay M, Mary B, Beaudoin N (2008) Conceptual basis, formalisations and parameterization of the STICS plant model. QUAE, Versailles
10. Cadoux S, Rich AB, Yates NE, Machet JM (2012) Nutrient requirements of *Miscanthus x gianteus*: conclusions from a review of published studies. Biomass Bioenergy 38:14–22

11. Cadoux S, Ferchaud F, Demay C, Boizard H, Machet JM, Fourdinier E, Preudhomme M, Chabbert B, Gosse G, Mary B (2013) Implications of productivity and nutrient requirements on greenhouse gas balance of annual and perennial bioenergy crops. GCB Bioenergy. doi:10.1111/gcbb.12065
12. Christian DG, Poulton PR, Riche AB, Yates NE, Todd AD (2006) The recovery over several seasons of 15N-labelled fertilizer applied to *Miscanthus x giganteus* ranging from 1 to 3 years old. Biomass Bioenergy 30:125–133
13. Clifton-Brown JC, Jones MB (1997) The thermal response of leaf expansion rate in genotypes of the C4-grasses Miscanthus: an important factor in determining the potential productivity of different genotypes. J Exp Bot 48:1573–1581
14. Clifton-Brown JC, Neilson B, Lewandowski I, Jones MB (2000) The modelled productivity of *Miscanthus x giganteus* (GREEF et DEU) in Ireland. Ind Crop Prod 12:97–109
15. Cosentino SL, Patanè C, Sanzone E, Copani V, Foti S (2007) Effects of soil water content and nitrogen supply on the productivity of *Miscanthus x giganteus* Greef et Deu. in a Mediterranean environment. Ind Crop Prod 25:75–88
16. de Souza AP, Arundale RA, Dohleman FG, Long SP, Buckeridge MS (2013) Will the exceptional productivity of *Miscanthus x giganteus* increase further under rising atmospheric CO_2? Agric For Meteorol 171:82–92
17. De Wit CT (1978) Simulation of assimilation, respiration and transpiration of crops. Pudoc, Wageningen
18. Dondini M, Hastings A, Saiz G, Jones M, Smith P (2009) The potential of Miscanthus to sequester carbon in soils; comparing field measurements in Carlow, Ireland to model predictions. GCB Bioenergy 1:413–425
19. Dohleman FG, Heaton EA, Arundale RA, Long SP (2012) Seasonal dynamics o above- and below-ground biomass and nitrogen partitioning in *Miscanthus*× *giganteus* and *Panicum virgatum* across three growing seasons. GCB Bioenergy 4:534–544
20. Dorsainvil F (2002) Evaluation par modélisation de l'impact environnemental des cultures intermédiaires sur les bilans d'eau et d'azote. Thèse, INA-PG, Paris, France
21. Greenwood DJ, Lemaire G, Gosse G, Cruz P, Draycott A, Neeteson JJ (1990) Decline in percentage N of C3 and C4 crops with increasing plant mass. Ann Bot 66:425–436
22. Hastings A, Clifton-Brown J, Wattenbach M, Mitchell CP, Smith P (2009) The development of MISCANFOR, a new *Miscanthus* plant growth model: towards more robust yield predictions under different climatic and soil conditions. GCB Bioenergy 1:154–170
23. Himken M, Lammel J, Neukirchen D, Czypionka-Krause U, Olfs HW (1997) Cultivation of Miscanthus under West European conditions: seasonal changes in dry matter production, nutrient uptake and remobilization. Plant Soil 189:117–126
24. Imsande J, Tourraine B (1994) N Demand and the regulation of nitrate uptake. Plant Physiol 105:3–7
25. Jing Q, Conijn SJG, Jongschaap REE, Binbradan PS (2012) Modeling the productivity of energy crops in different agro-ecological environments. Biomass Bioenergy 46:618–633
26. Jørgensen U, Mortensen M, Ohlsson C (2003) Light interception and dry matter conversion efficiency of miscanthus genotypes estimated from spectral reflectance measurements. New Phytol 157:263–270
27. Keating BA, Carberry PS, Hammer GL, Probert ME, Robertson MJ, Holzworth D, Huth NI, Hargreaves JNG, Meinke H, Hochman Z, McLean G, Verburg K, Snow V, Dimes JP, Silburn M, Wang E, Brown S, Bristow KL, Asseng S, Chapman S, McCown RL, Freebairn DM, Smith CJ (2003) An overview of APSIM, a model designed for farming systems simulation. Eur J Agron 18:267–288
28. Kiniry JR, Tischler CR, Van Esbroeck GA (1999) Radiation use efficiency and leaf CO2 exchange for diverse C4 grasses. Biomass Bioenergy 17:95–112
29. Lewandowski I, Clifton-Brown JC, Scurlock JMO, Huisman W (2000) Miscanthus European experience with a novel energy crop. Biomass Bioenergy 19:209–227
30. Miguez FE, Zhu X, Humphries S, Bollero GA, Long SP (2009) A semimechanistic model predicting the growth and production of the bioenergy plant *Miscanthus*× *giganteus*: description, parameterization and validation. GCB Bioenergy 1:282–296
31. Millard P, Hester A, Wendler R, Baillie G (2001) Interspecific defoliation responses of trees depend on sites of winter nitrogen storage. Funct Ecol 15:535–543
32. Nair SS, Kang S, Zhang X, Miguez FE, Izaurralde RC, Post WM, Dietze MC, Lynd LR, Wullschleger SD (2012) Bioenergy plant models: descriptions, data requirements, and future challenges. GCB Bioenergy 4:620–633
33. Ng TL, Eheart JW, Miguez F (2010) Modeling Miscanthus in the Soil and Water Assessment Tool (SWAT) to simulate its water quality effects as a bioenergy crop. Environ Sci Technol 44:7138–7144
34. Partala A, Mela T, Esala M, Ketoja E (2001) Plant recovery of ^{15}N-labelled nitrogen applied to reed canary grass grown for biomass. Nutr Cycl Agroecosyst 61:273–281
35. Plénet D, Lemaire G (1999) Relationships between dynamics of nitrogen uptake and dry matter accumulation in maize crops. Determination of critical N concentration. Plant Soil 216:65–82
36. Pogson M (2011) Modelling Miscanthus yields with low resolution input data. Ecol Model 222:3849–3853
37. Schjoerring JK, Bock JGH, Gammelvind L, Jensen CR, Mogensen VO (1995) Nitrogen incorporation and remobilization in different shoot components of field-grown winter oilseed rape (*Brassica napus* L.) as affected by rate of nitrogen application and irrigation. Plant Soil 177:255–264
38. Sinclair TR, Muchow RC (1999) Radiation use efficiency. Adv Agron 65:215–265
39. Strullu L, Cadoux S, Preudhomme M, Jeuffroy MH, Beaudoin N (2011) Biomass production, nitrogen accumulation and remobilisation by *Miscanthus x giganteus* as influenced by nitrogen stocks in belowground organs. Field Crop Res 121:381–391
40. Strullu L, Cadoux S, Beaudoin N, Jeuffroy MH (2013) Influence of belowground nitrogen stocks on light interception and conversion of *Miscanthus*× *giganteus*. Eur J Agron 47:1–10
41. Tayot X, Chartier M, Varlet-Grancher C, Lemaire G (1994) Potential above-ground dry matter production of Miscanthus in North-Centre France compared to sweet sorghum. Biomass Energy Environ Agric Ind 1:556–564
42. Teixeira EI, Moot DJ, Brown HE, Pollock KM (2007) How does defoliation management impact on yield, canopy forming processes and light interception of lucerne (*Medicago sativa* L.) crops? Eur J Agron 27:154–164
43. Thornton B, Millard P (1997) Increased defoliation frequency depletes remobilization of nitrogen for leaf growth in grasses. Ann Bot 80:89–95
44. Tuck G, Glendining MJ, Smith P, House JI, Wattenbach M (2006) The potential distribution of bioenergy crops in Europe under present and future climate. Biomass Bioenergy 30:183–197
45. van Heerwaarden LM, Toet S, Aerts R (2003) Nitrogen and phosphorus resorption efficiency and proficiency in six sub-arctic bog species after 4 years of nitrogen fertilization. J Ecol 91:1060–1070
46. van Heerwaarden LM, Toet S, van Logstestijn RSP, Aerts R (2005) Internal nitrogen dynamics in the graminoid *Molinia caerulea* under higher N supply and elevated CO_2 concentrations. Plant Soil 277: 255–264
47. Van Ittersum MK, Leffelaar PA, van Keulen H, Kropff MJ, Bastiaans L, Goudriaan J (2003) On approaches and applications of the Wageningen plant models. Eur J Agron 18:231–234
48. Willmott CJ (1981) On the validation of models. Phys Geogr 2:184–194